

# Effect of Sodium Dodecyl Sulphate (SDS) and Electrochemical Behavior of Electrodeposited PbO<sub>2</sub> on Nickel Substrate for Lead Acid Battery Application

Most. Sabina Yasmin<sup>a</sup>, Md. Saiful Islam<sup>a\*</sup>, C. M. Mustafa<sup>a</sup>,  
Md. Mayeedul Islam<sup>b</sup>, Md. Al-Amin<sup>a</sup> and Most. Ripa Khatun<sup>a</sup>

<sup>a</sup> Department of Applied Chemistry and Chemical Engineering, University of Rajshahi, Rajshahi, 6205, Bangladesh.

<sup>b</sup> Department of Chemistry, Rajshahi University of Engineering and Technology, Rajshahi, 6204, Bangladesh.

## Authors' contributions

*This work was carried out in collaboration among all authors. All authors read and approved the final manuscript.*

## Article Information

### Open Peer Review History:

This journal follows the Advanced Open Peer Review policy. Identity of the Reviewers, Editor(s) and additional Reviewers, peer review comments, different versions of the manuscript, comments of the editors, etc are available here: <https://www.sdiarticle5.com/review-history/84895>

Original Research Article

Received 12 January 2022  
Accepted 22 March 2022  
Published 08 April 2022

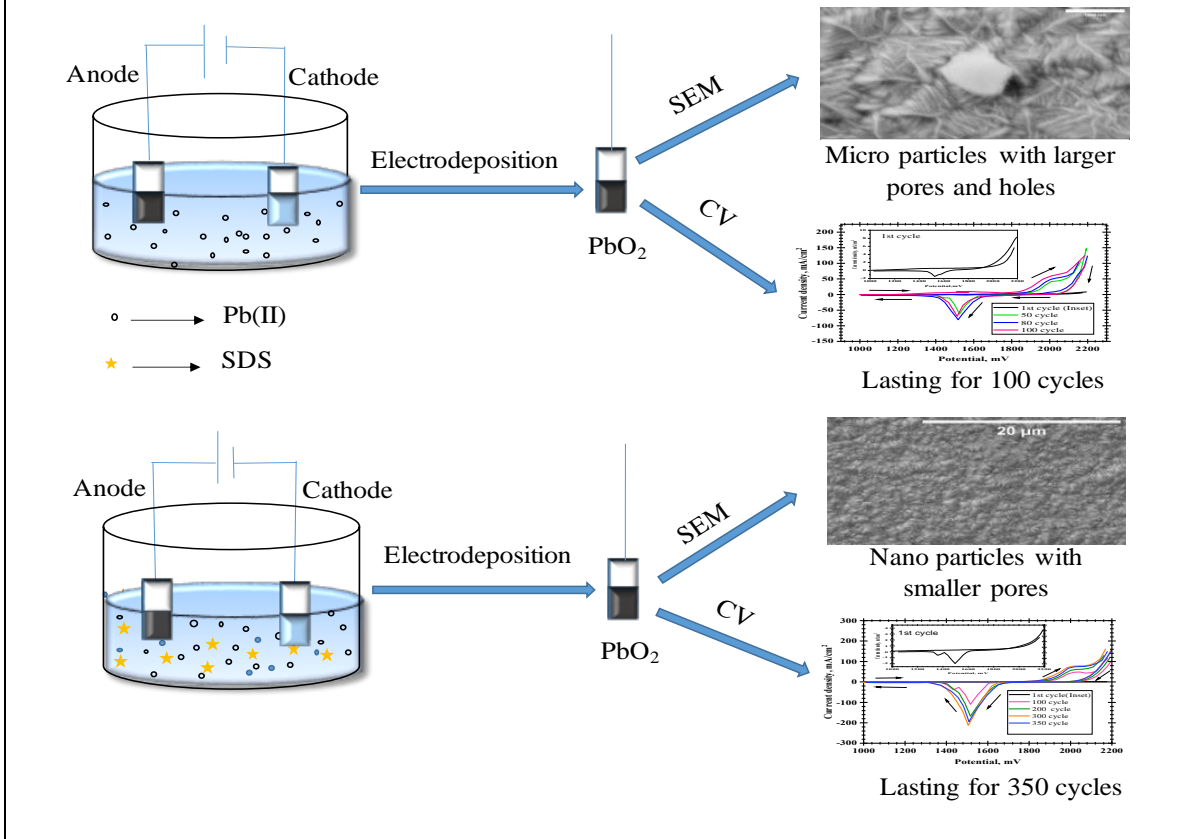
## ABSTRACT

An investigation has been made to electrodeposit PbO<sub>2</sub> anodically by galvanostatic deposition method on Ni substrate from highly alkaline lead acetate bath (0.2 M CH<sub>3</sub>(COO)<sub>2</sub> and 5 M NaOH) containing an anionic surfactant sodium dodecyl sulfate (SDS) for the application of lead-acid battery positive electrode. The electrodeposited PbO<sub>2</sub> was characterized sequentially by current efficiency and thickness measurement, visual and optical microscopic observation, cyclic voltammetry (CV) study, scanning electron microscopic (SEM), and X-ray diffraction (XRD) test. The results revealed that with the increase of SDS concentration the current efficiency as well as the thickness of PbO<sub>2</sub> deposits increased up to 100 mgL<sup>-1</sup> SDS and afterward it decreased. The morphological study showed that with the variation of SDS concentrations the morphology and particle size of deposited PbO<sub>2</sub> can be controlled. The electrochemical performance of the deposited samples in 4.7 M H<sub>2</sub>SO<sub>4</sub> solution (lead-acid battery electrolyte concentration) was investigated using cyclic voltammetry. In the absence of SDS, a pure PbO<sub>2</sub> deposit with a lower charge-discharge density and a lower stability (lasting up to 100 cycles) was formed. A small

\*Corresponding author: Email: saiful@ru.ac.bd, saiful005@gmail.com;

amount of SDS added to the electrolyte improved grain refinement of  $\alpha$ -PbO<sub>2</sub> with compact and small-grained crystals, increasing the PbO<sub>2</sub> film's stability (up to 350 cycles) and charge-discharge density in the battery environment.

### GRAPHICAL ABSTRACT



**Keywords:** Electrodeposition; alpha-lead dioxide; nickel substrate; lead-acid battery; SEM; XRD.

### 1. INTRODUCTION

In the world one of the most widely used energy is the electrical energy. The conversion of electrical energy to any other forms (mechanical energy, heat, and light) is easy and is transportable over long distances in a safe and efficient manner. However, a general problem associated with this is the difficulty in storage. Capacitors enable direct storage, but the quantities available are small in comparison to the demand for most applications. Secondary storage batteries are the best solution in this situation. Lead-acid, nickel-cadmium, nickel-metal hydride, and lithium-ion batteries are examples of secondary batteries. Among them, the most common rechargeable battery is the lead-acid battery (LAB), in which as positive and negative electrode PbO<sub>2</sub> pasted on a Pb grid and metallic spongy lead with a high surface are used respectively in an electrolyte (Approx. 5 M

sulfuric acid) [1-3]. Due to its availability, good stability, high discharge rate, adaptable performance, and ease of recycling, lead-acid batteries remain the most dominant electrical energy storage system nearly 150 years after their invention [2-5]. In lead-acid battery, spongy lead-coated lead and PbO<sub>2</sub> coated Pb is used as negative and positive electrode. Although lead-acid batteries are used in plenty in the field of rechargeable battery industry, this promising technology has some drawbacks that limit its application. The most significant disadvantage is its low energy density or specific energy per unit weight (30-40 Whkg<sup>-1</sup>) [5]. Grid typically materials for both anode and cathode are lead or lead alloys, and due to their high density, grids carry a significant portion of the battery weight. This is the primary reason for lead-acid batteries' low specific energy per unit weight. The use of lightweight substrates instead of a Pb grid will be a promising solution for that. A lot of research on

lightweight substrates Ti, [3,6,7], graphite felt [8], boron-doped diamond (BDD) [8,9], vitreous carbon electrode [7], Cu [10], platinum and Ni [11,12], gold [3,13] were used for electrodeposition of lead dioxide.

Yolshina et al. [14] deposited Pb film on a Cu and Cu-coated Ti-substrate for the positive electrode and showed that it provides higher discharge current density than conventional one. Later, to minimize the problems of low utilization positive active materials (PAM) and high internal resistance of positive electrode in LAB lead foam alloy were electrodeposited on a copper foam substrate [15]. The corrosion resistance of the copper foam substrate affected by the thickness of the lead coating. Furthermore, when compared to the cast grid battery, the lead foam collectors increased the PAM utilization and charge discharge performance by (19-36) percent. There are two polymorphs of PbO<sub>2</sub> crystals: tetragonal  $\beta$ -PbO<sub>2</sub>, and orthorhombic  $\alpha$ -PbO<sub>2</sub> and their abundance is determined by type of substrate and deposition conditions [2,16]. In general,  $\alpha$ -PbO<sub>2</sub> obtained from an alkaline solution with a more compact structure has better particle contact than  $\beta$ -PbO<sub>2</sub> which is obtained from an acidic medium. However, in dilute H<sub>2</sub>SO<sub>4</sub>  $\beta$ -PbO<sub>2</sub> has superior catalytic activity [17,18].

Alexander Velichenko prepared sub micrometric and nanometric electrodeposited PbO<sub>2</sub> anode in presence of potassium salt of nonafluorobutanesulfonic acid (C<sub>4</sub>F<sub>9</sub>SO<sub>3</sub>K) from nitrate electrolytes for electrocatalytic activity. They found that the addition of C<sub>4</sub>F<sub>9</sub>SO<sub>3</sub>K in the electrolyte solution of PbO<sub>2</sub> electrodeposition lead to an inhibition of the oxygen evolution process and increase the rate of electrochemical conversion of 4-chlorophenol to aliphatic compounds three times [18].

Cao et al. [19] investigated single-crystals of lead dioxide nanorods from an alkaline lead nitrate solution containing cetyltrimethylammonium bromide (CTAB). Xi et al. [20] prepared PbO<sub>2</sub> hollow spheres of sub-micrometer-sized (200-400 nm) from an alkaline solution of lead nitrate in the presence of PVP. In our previous work [21] we prepared an electrodeposited PbO<sub>2</sub> electrode on the nickel substrate from acidic lead nitrate medium in the presence of SDS and NaF and discovered that the presence of NaF and SDS in the depositing bath facilitated in grain refinement of the deposit. We found that Compact and small-grained deposits with a higher proportion of  $\beta$ -PbO<sub>2</sub> were formed, and they lasted for 300

cycles with a relatively higher charge-discharge density in 4.7 molL<sup>-1</sup> H<sub>2</sub>SO<sub>4</sub> (battery electrolyte condition). In this study, we prepared an electrodeposited PbO<sub>2</sub> on Ni substrate from an alkaline lead acetate medium in the presence of SDS as a surfactant and studied its effect on the morphology, crystalline structure, and electrochemical performance of the prepared PbO<sub>2</sub>.

## 2. EXPERIMENTAL

### 2.1 Substrate

Commercially pure (99.9%) nickel sheets with a thickness of 0.5 mm were cut into 1 cm × 4 cm coupons and used as substrates for PbO<sub>2</sub> electrodeposition. Coupons were polished with SiC abrasive paper up to 1200 grit, washed with liquid soap solution, and immersed in an aqueous 1 percent NaOH solution for 5 minutes. These were then washed with distilled water and dried in the open air. Insulating paint was applied to both sides of the coupons, leaving a 1 cm<sup>2</sup> space exposed at one end for experiment. A small portion at the other end were also left bare for electrical contact. The coupons were then dried in an oven at 80°C for 1 hour for curing and removal of moisture. The coupons were weighted properly with an analytical balance after cooling it to room temperature and stored in a desiccator usually contains silica gel for the electrodeposition experiment.

### 2.2 Solutions

Just before running any electrodeposition experiment, the prepared Ni coupon was dipped into 0.1 M H<sub>2</sub>SO<sub>4</sub> for 10 minutes for surface activation. The reagents used in this study included lead acetate (Qualikems, India), sulfuric acid (BDH, England), NaOH (E. Merck, India), sodium dodecyl sulfate (Loba Chemie, India), The Pb(CH<sub>3</sub>COO)<sub>2</sub> concentrations used in this study were 0.2 M, NaOH 5 M and SDS concentrations range from 10 mgL<sup>-1</sup> to 500 mgL<sup>-1</sup> respectively.

### 2.3 Electrodeposition of PbO<sub>2</sub>

PbO<sub>2</sub> has electrodeposited Galvano static mode by using a DC Power supply (Model PS 303, Loadstar Electronics, Taiwan). A 250 mL Pyrex glass beaker with 200 mL electrolyte was put on a magnetic stirrer with hot plate as the electrolytic cell (Model; MS300HS, Brand: Mtops Korea). Before and after each deposition the solution pH was measured. The positive terminal

of the power source was connected with a prepared nickel coupon (anode) while the negative terminal was connected to another clean coupon. They were placed in the cell solution in parallel, 2cm apart, with the exposed surface well immersed in the electrolyte and the crocodile clips for electrical contact well connected. For measuring current, a digital multimeter with an ammeter of zero resistance of Sanwa, multimeter, Model 300D, China) was attached in series. When a controlled current was applied the oxidation of  $Pb^{2+}$  ions were appeared and deposited as  $PbO_2$  on the anode. After electrodeposition for the recommended condition, the deposited coupon was carefully cleaned with distilled water and dried in an oven at  $80^\circ C$  for one hour. The weight was then measured correctly at room temperature. The difference in the weight of the coupon after and before electrodeposition was used to calculate the amount of  $PbO_2$  deposited. Using faraday's law of electrolysis, the current efficiency and thickness of the deposition were calculated. To ensure reproducibility, each experiment was repeated at least three times.

#### 2.4 Determination of Morphology and Crystal Structure

A high-resolution Optical Microscope (OM) (ACME 40x-640x Digital Metallurgical Microscope, India) and Scanning Electron Microscope (SEM) (FEI Inspect S50, Oregon, USA) were used to characterize the surface microstructure. Before taking images, a conductive coating (gold) was sputtered onto the coated samples. Before being subjected to XRD analysis, the lead dioxide deposits were cleaned with acetone, dried, removed from the surface, and ground in a mortar. The powder was then compressed and placed on glass for diffraction. A Philips X'pret MPD diffractometer with a Cu K radiation ( $\lambda = 1.5418$ ); generator settings: 40 kV, 30 mA; step size:  $0.02^\circ$ ; and  $2\theta$  range:  $20^\circ$ - $80^\circ$  was used for the X-ray diffraction analysis.

#### 2.5 Cyclic Voltammetry (CV) Characterization

A Gill AC Impedance Analyzer (ACM Instruments, England) with three electrode cell arrangement was used for CV experiment in which deposited  $PbO_2$ , SSE with Luggin capillary probe, and Pt wire gauge were used as a working electrode (WE), reference electrode, and counter electrode respectively. All voltammetry experiments were performed under static conditions in 4.7 M  $H_2SO_4$  maintaining  $30^\circ C$ . The charge and discharge

densities were calculated dividing the anodic and cathodic peak area by scan rate and the discharge efficiency was the ratio of the discharge density and charge density multiplied by 100.

### 3. RESULTS AND DISCUSSION

#### 3.1 Electrolysis

Fig.1 shows the current efficiency (CE) and thickness of electrodeposited  $PbO_2$  prepared with and without anionic surfactants SDS. The surfactant-free bath yields  $PbO_2$  with a CE of 96 percent and thickness of  $45.1 \mu m$ . when the surfactant is added, the CE increases to a maximum (marked as optimum surfactant concentration) (for anionic surfactant SDS) before decreasing with the addition of excess surfactant. In presence of SDS, the oxygen evolution decreases thus the CE increases. [22]. But at a high concentration of SDS the current efficiency and thickness decrease due to the blocking effect.

From the Fig.1, it is clear that with increasing SDS concentration current efficiency and thickness increase up to 200 mg/L afterward decreasing the CE and thickness.

Fig. 2 shows CV of deposited  $PbO_2$  in 4.7 M  $H_2SO_4$ . The voltammograms were started anodically at 1000 mV at 30 mV/s scan rate and extended up to 2200 mV. The potential was measured concerning saturated Ag/AgCl electrodes (SSE). The  $PbO_2$  was electrodeposited on the Ni-substrate from a solution containing 0.2 M  $Pb(CH_3COO)_2$  in 5 M aqueous NaOH at  $55^\circ C$  temperature using 10  $mA/cm^2$  current density in presence of 0, 10, 50, 100, 200, and 500 mg/L SDS. As shown in the figure, during the anodic scan of all the  $PbO_2$  electrodes a steady current rise was observed after 2000 mV without the appearance of any peak. As  $PbO_2$  was already electrodeposited on the electrode, the current was mainly due to oxygen evolution reaction [23-26]. During the reverse sweep, two well-defined peaks were observed due to  $PbO_2$  to  $PbSO_4$  conversion at around 1560 mV and 1430 mV for  $PbO_2$  deposited from 50, and 100 mg/L SDS containing solution and other  $PbO_2$  electrode show only one peak for the conversion of  $\alpha$   $PbO_2$  to  $PbSO_4$ . However, it could be seen that the reduction potential shifted more negative direction with increasing of SDS concentration up to 100 mg/L but decreased at 200 mg/L and 500 mg/L SDS

concentration. In addition, the amount of charge involved during PbO<sub>2</sub> reduction using the electrode constructed at an SDS concentration of 100 mg/L appeared to be the highest of the six samples. This implies that the PbO<sub>2</sub> electrode

deposited from 100 mg/L SDS may contain more active materials involved in sulfuric acid discharge cycles. Since, the SEM and XRD results revealed this, 100 mg/L SDS was used as the optimum condition for my experiment.

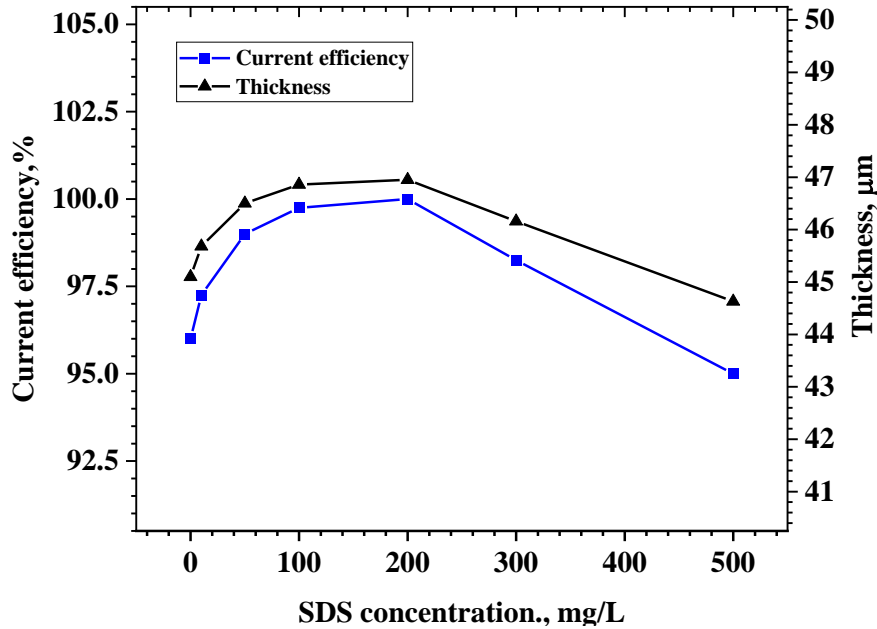


**Fig. 1.** Current efficiency and thickness of PbO<sub>2</sub> electrodeposition on Ni-substrate from 0.2 M lead acetate and 5 m NaOH solution containing 0.10, 50, 100, 200, and 500 mg/L SDS. The deposition was carried out at 10 mA/cm<sup>2</sup> current density, 55°C temperature for 60 minutes

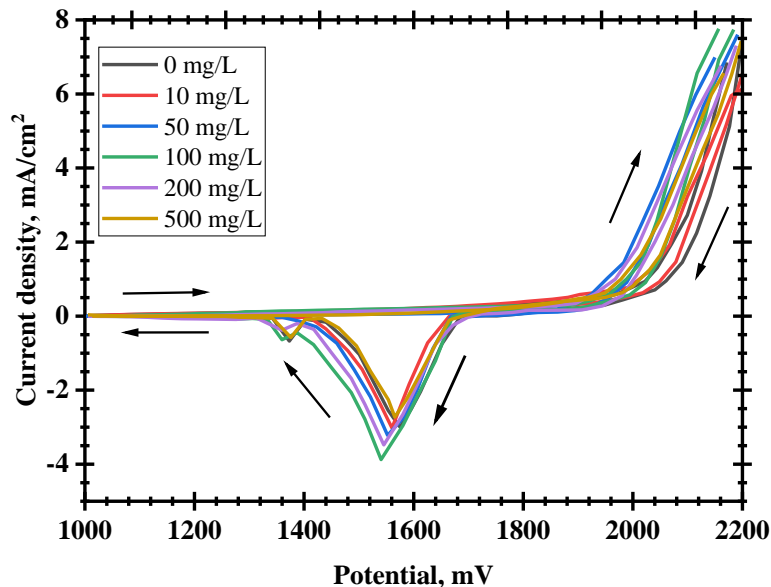


**Fig. 2.** CV plots of PbO<sub>2</sub> deposited from 0.2 M Pb and 5 M NaOH solution containing 0, 10, 50, 100, 200 and 500 mg/L SDS. The deposition parameters were same as Fig.1, The CV was carried out in 4.7 M H<sub>2</sub>SO<sub>4</sub> solution at 30 mV/s scan rate maintaining temperature at 30°C

### 3.2 Cyclic Voltammetry (CV) /Charge Discharge Cycle Life

A porous structure facilitates the better utilization of  $\text{PbO}_2$  active materials; however, excessive porosity reduces particle connectivity, reducing the active materials' discharge capacity significantly [27]. The CV results, clearly implies that the electrochemical performance of micro/nano-structured  $\text{PbO}_2$  thin films made of small nanoparticles is excellent. Cyclic voltammetry provides more information about electrochemical reaction mechanisms, stability, performance, and side reaction conditions. All CV experiments were carried out in 4.7 mol/L  $\text{H}_2\text{SO}_4$  (approximate concentration of  $\text{H}_2\text{SO}_4$  in the lead-acid battery) at 30 °C temperature and voltage from 1000 mV - 2200 mV at 30 mV/S scan rate to better understand the phenomena occurring in lead-acid battery conditions.

We compared the charge/discharge cycling life of two  $\text{PbO}_2$  electrodes that were prepared electrochemically at 0 mg/L SDS and 100 mg/L SDS Ni substrate, and then characterized the morphology and microstructure of those thin-film using SEM, Optical Microscopic Examination, and XRD to confirm the viewpoint [28].

Fig. 3 (a) shows the CV graphs of electrodeposited  $\text{PbO}_2$  in 4.7M  $\text{H}_2\text{SO}_4$ . The voltammograms were started anodically at 1000 mV at a scan rate of 30 mV/s scan and extended up to 2200 mV. The potential was measured with respect to saturated Ag/AgCl electrodes (SSE). The electrodeposition of  $\text{PbO}_2$  on the Ni-substrate was made from a solution containing 0.2 M  $\text{Pb}(\text{CH}_3\text{COO})_2$  in 5 M aqueous NaOH at 55°C temperature using 10 mA/cm<sup>2</sup> current density in absence of SDS additives. Before running successive cycles, open circuit potential (OCP) was noted up to the stable which was 1556 mV. The oxidation of PbO to  $\text{Pb}_3\text{O}_4$  ( $2\text{PbO} \cdot \text{PbO}_2$ ) (up to 1200 mV) [29] and  $\text{Pb}_3\text{O}_4$  to  $\text{PbO}_2$   $\text{Pb}_3\text{O}_4$  to  $\text{PbO}_2$  [16] may result in a small amount of current (~0.2 mA/cm<sup>2</sup>) in the potential range between 1000 mV and 1850 mV (beginning of  $\text{O}_2$  evolution) during the anodic scan of the first cycle (elaborated in the inset). After 2000 mV current started to rise sharply due to oxygen evolution reaction [23-26]. During the cathodic scan of the 1st cycle, two well-defined small peaks at 1560 mV and 1430 mV were reduced of  $\text{PbO}_2$  to  $\text{PbSO}_4$  [16].  $\text{PbO}_2$  can exist as  $\alpha$ - $\text{PbO}_2$  (orthorhombic structure) and  $\beta$ - $\text{PbO}_2$  (tetragonal structure), and their relative amounts of deposition during  $\text{PbO}_2$  formation depend on

the pH of the electrolytic medium and other factors as reported in the literature [16,30]. According to the literature reports [11,31] mixtures of  $\alpha$ - and  $\beta$ - $\text{PbO}_2$  electrodeposit from acidic medium, but in alkaline medium only  $\alpha$ - $\text{PbO}_2$  forms [32]. It has been reported [33] that conversion of  $\alpha$ - $\text{PbO}_2$  to  $\text{PbSO}_4$  happens at relatively higher positive potential compared to that of  $\beta$ - $\text{PbO}_2$ . So, in the cathodic scan of all cases, peaks at larger positive potential were due to the reduction of  $\alpha$ - $\text{PbO}_2$ , and less positive potential were due to the reduction of  $\beta$ - $\text{PbO}_2$  to  $\text{PbSO}_4$  respectively [34]. In the present work the  $\text{PbO}_2$  electrodeposition was carried out in alkaline media, so deposit was mainly  $\alpha$ - $\text{PbO}_2$ . However, cyclic voltammetry was carried out in a highly acidic medium (4.7M  $\text{H}_2\text{SO}_4$ ), so there might be the instantaneous conversion of some pure  $\alpha$ - $\text{PbO}_2$  to  $\beta$ - $\text{PbO}_2$ . The 50<sup>th</sup> cycle shows the anodic peak current of 38 mA/cm<sup>2</sup> at approx. 2004 mV due to the conversion of  $\text{PbSO}_4$  to  $\text{PbO}_2$  that merged with oxygen generation reaction after 2140 mV [21]. During the cathodic sweep two peaks at 1526 mV and 1446 mV with peak current densities of 62 mA/cm<sup>2</sup> and 10 mA/cm<sup>2</sup> were for the conversion of  $\alpha$ - $\text{PbO}_2$  to  $\text{PbSO}_4$  and  $\beta$ - $\text{PbO}_2$  to  $\text{PbSO}_4$  respectively [34]. The 80<sup>th</sup> cycle of anodic scan shows a peak at the same position as the 50<sup>th</sup> cycle but with a higher current density (48 mA/cm<sup>2</sup>) due to  $\text{PbSO}_4$  conversion to  $\text{PbO}_2$ . The corresponding cathodic sweep demonstrates cathodic peaks shifted to negative potential than 50<sup>th</sup> cycle at 1507 mV with a peak current density of 75 mA/cm<sup>2</sup> and  $\beta$ - $\text{PbO}_2$  merge with  $\alpha$ - $\text{PbO}_2$ . As the cyclic voltammogram is carried out in an acidic medium (4.7M  $\text{H}_2\text{SO}_4$ )  $\text{PbSO}_4$  is mainly oxidized to  $\beta$ - $\text{PbO}_2$ . So, with increasing cycle number amount of  $\beta$ - $\text{PbO}_2$  also increases on the surface of the electrode. So, there is always a mixture of  $\alpha$ - $\text{PbO}_2$  and  $\beta$ - $\text{PbO}_2$  present on the surface. That is why with increasing cycle number  $\text{PbO}_2$  to  $\text{PbSO}_4$  conversion peak shifts to the negative direction in Fig.3(a) [35]. Both the anodic and cathodic peak current densities were lower in the case 100<sup>th</sup> cycle than in the 80<sup>th</sup> cycle and a broad and swallow peak between 1420-1800 mV was found for the oxidation of Ni to NiO(OH) [21,36,37]. Fig. 3b. illustrates the effect of cycle numbers on charge ( $\text{PbSO}_4$  to  $\text{PbO}_2$ ) density, discharge ( $\text{PbO}_2$  to  $\text{PbSO}_4$ ) density and discharge efficiency. The graph shows that the charge and discharge densities slowly increase with cycle number until the 60th cycle, afterwards rapidly increase. Because at starting the charging cycle the surface was completely made

up of PbO<sub>2</sub> film, no oxidation of PbSO<sub>4</sub> to PbO<sub>2</sub> occurred. However, PbSO<sub>4</sub> converted to PbO<sub>2</sub> during the subsequent discharge cycle. As a result, the lower charge density was obtained than the corresponding discharge density at the start of the CV. With the increase of cycle number, a more porous PbO<sub>2</sub> with higher surface area formed, allowing H<sup>+</sup>, HSO<sub>4</sub><sup>-</sup>, and H<sub>2</sub>SO<sub>4</sub> to interact with the electrode material. The charge density and discharge density increased as a result, [35]. Also, through the more porous structure Ni come in contact with H<sub>2</sub>SO<sub>4</sub>, corroded and goes to solution. As a result, the PbO<sub>2</sub> electrode become damaged.  $\alpha$ -PbO<sub>2</sub>,  $\beta$ -PbO<sub>2</sub>, and PbSO<sub>4</sub> have densities of 9.87 g/cm<sup>3</sup>, 9.3 g/cm<sup>3</sup>, as well as 6.29 g/cm<sup>3</sup>, respectively [36]. During successive cycling for the expansion and contraction of volume a stress developed on the PbO<sub>2</sub> which is responsible for parting away from the substrate at larger cycles in H<sub>2</sub>SO<sub>4</sub>. The beginning discharge efficiency above 110 percent significantly dropped as the cycle number increased. This means that in the absence of PbSO<sub>4</sub>, the PbO<sub>2</sub> film's initial discharge (PbO<sub>2</sub> to PbSO<sub>4</sub>) density was greater than the corresponding charge (PbSO<sub>4</sub> to PbO<sub>2</sub>) density. Because of the increased oxygen evolution from the active surface, discharge efficiency decreased as the cycle number increased. In the latter stages of cycling, the abundant oxygen formation merged with the charge current density, contributing to a decrease in discharge efficiency. This implies that the surface area of the PbO<sub>2</sub> film was reduced as a result of a significant amount of PbO<sub>2</sub> falling apart from the Ni substrate. OCP drops to 235 mV after the 100<sup>th</sup> cycle.

Fig. 4(a) depicts the results of a CV results obtained from a PbO<sub>2</sub> electrode deposited on a Ni substrate under the same conditions as in Fig. 3 (a). but with the incorporation of 100 mg/L SDS in the electrolyte. Cyclic voltammetry condition was also the same as Fig. 3 (a) The cyclic voltammetry was continued up to 350 cycles. Afterward, it was discontinued due to the rapid deterioration of the deposited surface. Before starting successive cycle open circuit potential (OCP) was recorded to be stable which was 1560 mV. OCP dramatically dropped after the 350<sup>th</sup> cycle The voltammogram for 1<sup>st</sup>, 100<sup>th</sup>, 200<sup>th</sup>, 300<sup>th</sup> and 350<sup>th</sup> cycles are shown in Fig.4 (a) All of these have distinct anodic and cathodic peaks with higher current densities when compared to Fig. 3(a), the corresponding cycles when deposited on Ni substrate. Each case Peak shifted to more negative potential and peak

current also increased up to 300 cycles. After 350 cycles both anodic and cathodic peak current decreased and Ni oxidation current was found and Ni goes to the solution. After the 350 cycles, the open circuit potential decreased to 280 mV as the nickel surface was exposed to the sulfuric acid solution. In H<sub>2</sub>SO<sub>4</sub> media, the 300<sup>th</sup> cycle was completed without any nickel corrosion. This indicates that the nickel surface has completely covered with the PbO<sub>2</sub> film. Even after 60 cycles, PbO<sub>2</sub> could not prevent base Ni from corrosion in the absence of SDS (Fig. 3a), whereas with additive (SDS), the protection limit was above 350 cycles. Surprisingly, no anodic current for nickel oxidation up to 350 cycles, indicating the surface's remarkable stability. The charge and discharge behavior are as usual as described in Fig.3 (b).

### 3.3 Electrochemical Property Correlation with Surface Microstructure

Optical Microscopic Examination and Scanning Electron microscopic Examination (SEM) were used to examine the size and morphology of the synthesized films.

Fig. 5 shows the Optical Microscopic Examination of the electrodeposited PbO<sub>2</sub>. From the microscopic figure, it is clear that in the absence of SDS (Fig. 6(b)) non uniform and larger particle-sized agglomerated particles with holes and pores are present on the surface. With increasing the concentration of the SDS amount of agglomerated particles and holes is decreased. At 100 and 200 mg/L SDS concentration uniformly deposited non-agglomerated particles are found. At 500 mg/L SDS, the agglomerated particles coalesce into aggregated PbO<sub>2</sub> particles and more compact deposits are formed. All of these are also supported by SEM, XRD, and Cyclic voltammetry (CV) experiments.

From Fig. 6, it can be found the SDS concentration affects the morphology of electrodeposited PbO<sub>2</sub>. PbO<sub>2</sub> prepared in the absence of SDS are noticeably larger (microstructures) than those prepared with the surfactant SDS (nanostructures). The sample with no SDS consists of larger-sized flower-like particles of the highest and lowest particle range is 3  $\mu$ m - 542 nm (Fig. 6a), which are themselves contained smaller non-uniform rod-like crystallites of the biggest grain with 163 nm long and 15 nm wide, and the smallest one with 41 nm long and 6 nm wide (Fig. 6b) with several holes and pores. In the presence of SDS more

compact and decreased particle-sized  $\text{PbO}_2$  was obtained. The  $\text{PbO}_2$  at 50 mg/L SDS (Fig. 2b) consists of flower-like particles of the highest and lowest particle range is  $1.8 \mu\text{m}$  -  $272\text{nm}$  composed with a relatively smaller sized rod-like particles of the biggest grain with  $33 \text{ nm}$  long and  $6 \text{ nm}$  wide, and the smallest one with  $16 \text{ nm}$  long and  $6 \text{ nm}$  wide (Fig. 6b) with less pore and holes. In the case of  $100 \text{ mg/L}$  SDS,  $\text{PbO}_2$  particles are composed of smaller flower-like grain in the range of ( $1.2 \mu\text{m}$  -  $240 \text{ nm}$ ) comprise of ( $16\text{-}28$ )  $\text{nm}$  length and  $6 \text{ nm}$  wide particles (Fig. 6c). For  $200 \text{ mg/L}$  SDS containing  $\text{PbO}_2$  sample consists of ( $28\text{-}12$ )  $\text{nm}$  length and  $6 \text{ nm}$  wide. In the case of  $500 \text{ mg/L}$ , SDS containing  $\text{PbO}_2$  the smaller sized particles ( $1 \mu\text{m}\text{-}240 \text{ nm}$ ) particles comprised with ( $16\text{-}28$ )  $\text{nm}$  length and  $6 \text{ nm}$  wide particles coalescence and form aggregates of  $\text{PbO}_2$  particles of ( $5\text{-}34$ )  $\mu\text{m}$ . The presence of SDS smoothed and adhered the lead dioxide surface to the substrate, resulting in improved  $\text{H}_2\text{SO}_4$  cycling performance. Because the thicknesses of the two deposits (without and with SDS) were essentially equal ( $79 \mu\text{m}$ ), the lead dioxide film deposited from the SDS-containing solution was expected to have much more layers than the one deposited without SDS because the latter had a larger grain size. As a result, electrolytes such as  $\text{H}^+$  and  $\text{HSO}_4^-$  are much less

able to penetrate the  $\text{PbO}_2$  film deposited in the presence of SDS during the  $\text{PbSO}_4$  to  $\text{PbO}_2$  to  $\text{PbSO}_4$  conversion process, with  $\text{H}_2\text{SO}_4$  exhibiting the highest stability, as previously observed in cyclic voltammetry experiments.(Fig. 3a and Fig. 4a).

The phase composition of electrodeposited  $\text{PbO}_2$  samples was determined using X-ray diffraction. Generally,  $\text{PbO}_2$  can be found in two forms: tetragonal  $\beta\text{-PbO}_2$  and orthorhombic  $\alpha\text{-PbO}_2$ . The structure of  $\alpha\text{-PbO}_2$  is much more compact than those of more porous  $\beta\text{-PbO}_2$ , resulting in better particle interaction.

Fig. 7 illustrates the XRD graph of  $\text{PbO}_2$  electrodeposited on Ni substrate from an alkaline ( $5\text{M}$ ) solution  $0.2 \text{ M Pb}(\text{CH}_3\text{COO})_2$  containing 0, 50, 100, 200, and  $500 \text{ mg/L}$  SDS on Ni substrate. Only the characteristic peaks of  $\alpha\text{-PbO}_2$ , denoted by the Miller number were noticed for all the deposited samples, as shown in Fig. 7. According to previous research,  $\text{PbO}_2$  deposited from acidified  $\text{Pb}(\text{II})$  solution consists only  $\beta\text{-PbO}_2$ , but in alkaline solution,  $\alpha\text{-PbO}_2$  is the dominant form [39, 40].  $500 \text{ mg/L}$  SDS shows a higher degree of crystallinity while  $0 \text{ mg/L}$  SDS containing electrode shows a lower degree of crystallinity.

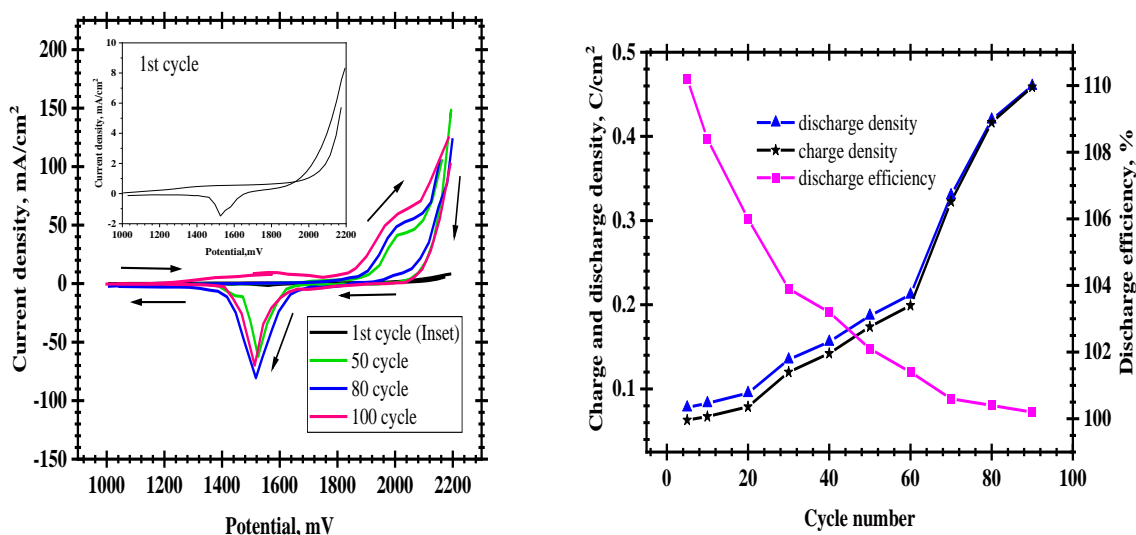


**Fig. 3 (a). Cyclic voltammetry and (b) Charge density, discharge density and discharge efficiency of deposited  $\text{PbO}_2$  in  $4.7 \text{ M H}_2\text{SO}_4$  at  $30^\circ\text{C}$  temperature. The electrodeposition of  $\text{PbO}_2$  film was carried out from an alkaline ( $5\text{M NaOH}$ )  $0.2 \text{ M Pb}(\text{CH}_3\text{COO})_2$  solution at  $10 \text{ mA/cm}^2$  current density and  $55^\circ\text{C}$  for  $90 \text{ min}$**



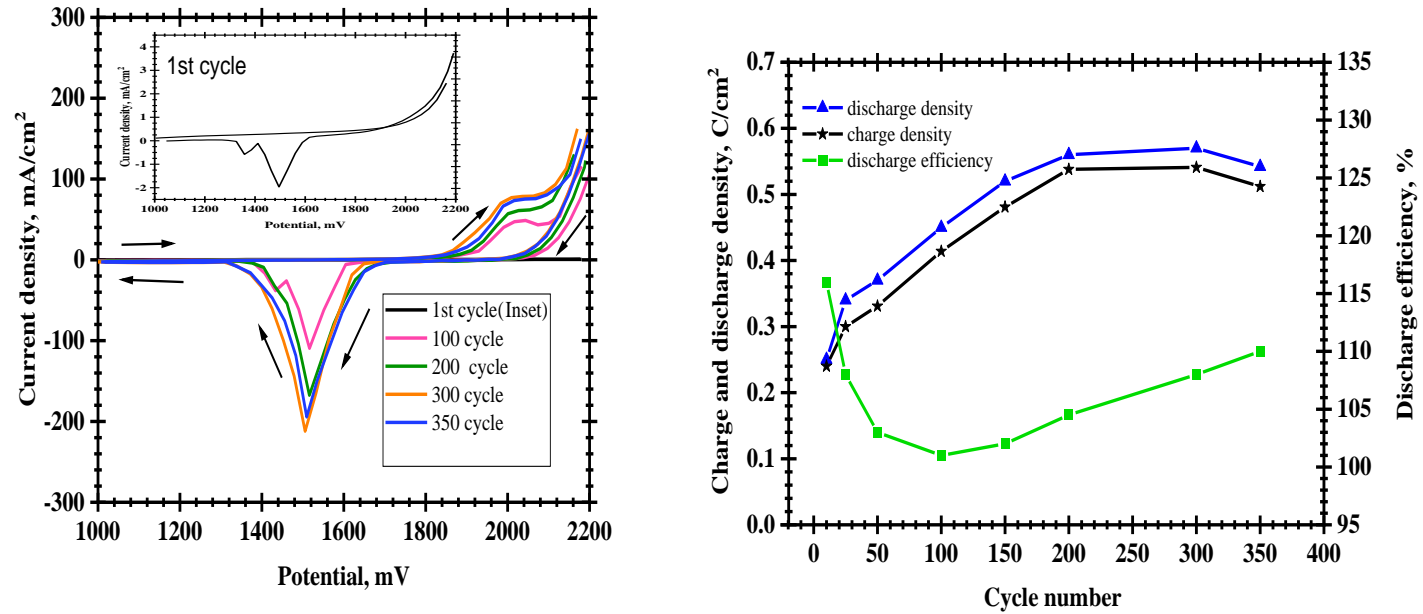
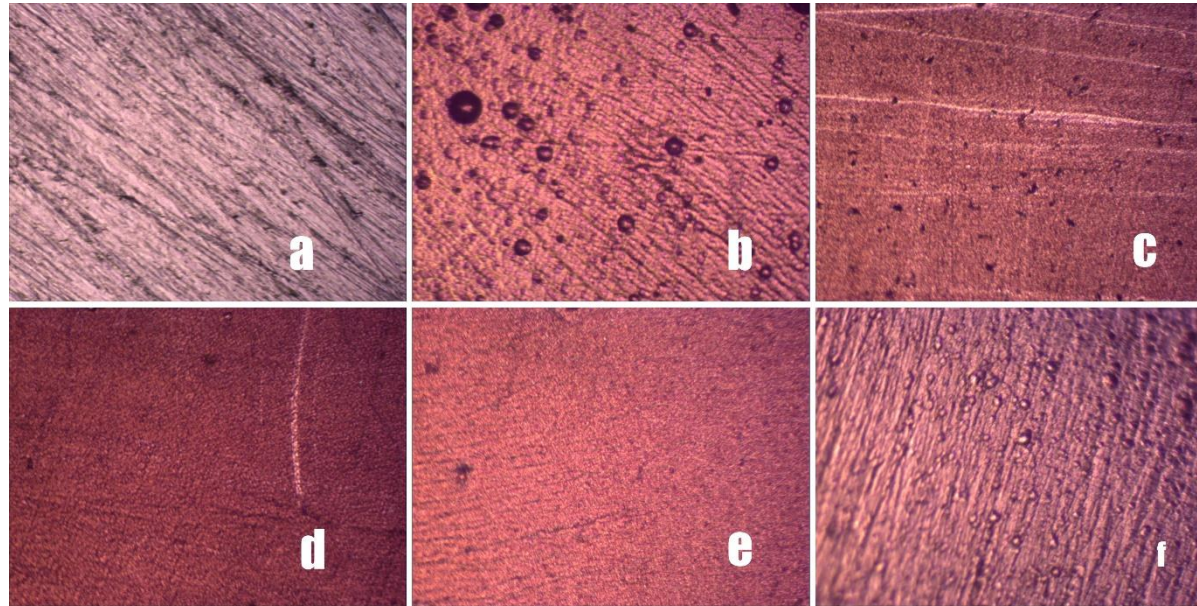
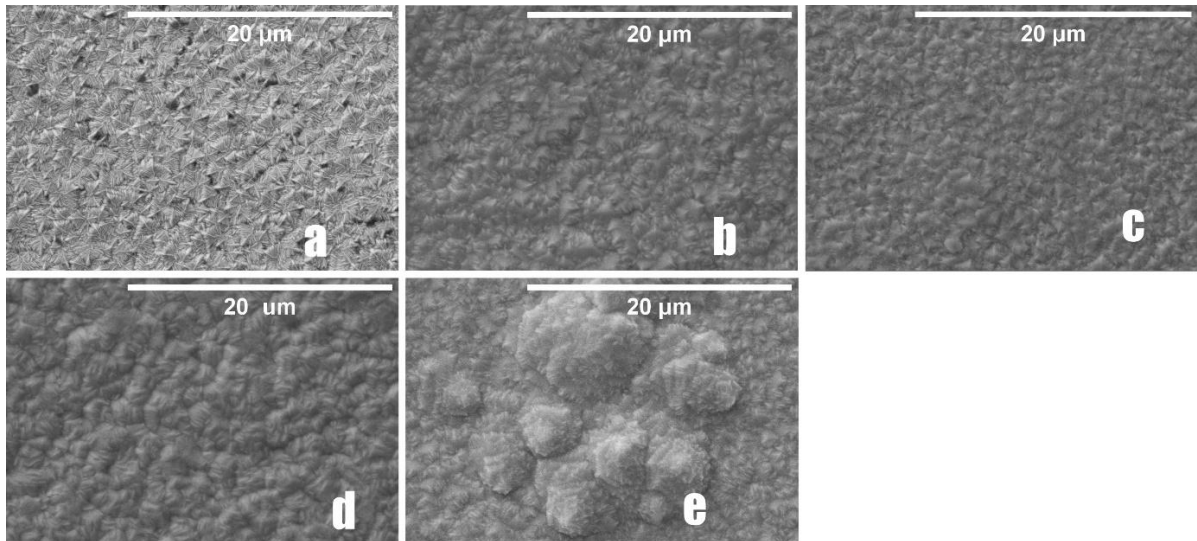


Fig. 4 (a) Cyclic voltammetric results and (b) Charge-discharge densities and discharge efficiency against cycle number of PbO<sub>2</sub> in 4.7 M H<sub>2</sub>SO<sub>4</sub> at room temperature, Electrodeposition of PbO<sub>2</sub> film was carried out from an alkaline (5M NaOH) 0.2 M Pb(CH<sub>3</sub>COO)<sub>2</sub> solution in presence of 100 mg/L SDS at 10 mA/cm<sup>2</sup> current density and 55°C for 90 min



**Fig. 5. Optical Microscopic picture of electrodeposited PbO<sub>2</sub> from 0.2M Pb(CH<sub>3</sub>COO)<sub>2</sub> solution in 5 M NaOH. The deposition current density was 10 mA/cm<sup>2</sup> for constant 36 coulombs of electricity at 55°C (a) Pure Ni sheet (b)in absence of SDS (c) in presence of 50 mg/L SDS (d) in presence of 100 mg/L SDS (e) in presence of 200 mg/L SDS (f) in presence of 500 mg/L SDS. Magnification was 400X**



**Fig. 6 Scanning Electron Microscopic (SEM) picture of electrodeposited PbO<sub>2</sub> from 0.2M Pb(CH<sub>3</sub>COO)<sub>2</sub> solution in 5 M NaOH. The deposition current density was 10 mA/cm<sup>2</sup> for constant 36 coulombs of electricity at 55°C (a) in absence of SDS (b) in presence of 50 mg/L SDS (c) in presence of 100 mg/L SDS (d) in presence of 200 mg/L SDS (e) in presence of 500 mg/L SDS. Magnification was 10000x**

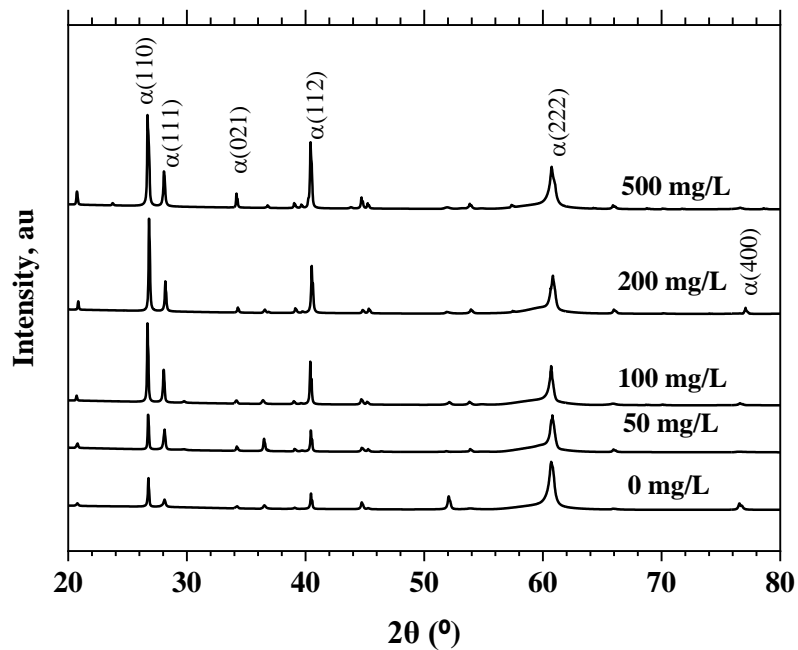


**Fig. 7. X-ray diffractograms of PbO<sub>2</sub> electrodeposited on Ni-substrate from an electrolyte containing 0.2M lead acetate in 5M NaOH at 10 mA/cm<sup>2</sup> current density for the thickness of 74 µm for all cases at 55°C at different concentrations of SDS**

#### 4. CONCLUSIONS

PbO<sub>2</sub> electrode was electrodeposited on the nickel substrate using Galvano static mode from alkaline Pb(CH<sub>3</sub>COO)<sub>2</sub> containing SDS additive for using as a positive electrode in a lightweight LAB.

The following are the findings of the study:

- SDS concentration had a much stronger influence on the surface morphology. It has been shown that lead dioxide electrodeposited from 100 mg/L SDS on Ni substrate had more uniform nanocrystals.

- From the XRD data, it was seen that the presence of SDS increased the  $\alpha$  PbO<sub>2</sub> into the PbO<sub>2</sub> electrode.
- From the cyclic voltammetry studies, it was found that the higher oxygen evolution potential and lower oxygen evolution peak current were obtained for 100 mg/L SDS-containing electrodes. And also increased number of the charged discharged cycle was obtained for 100 mg/L SDS on Ni. In the case of 100 mg/L SDS addition in the electrolyte solution, the stability became 4.5 times higher than 0 mg/L SDS.

## DISCLAIMER

The products used for this research are commonly and predominantly use products in our area of research and country. There is absolutely no conflict of interest between the authors and producers of the products because we do not intend to use these products as an avenue for any litigation but for the advancement of knowledge. Also, the research was not funded by the producing company rather it was funded by personal efforts of the authors.

## COMPETING INTERESTS

Authors have declared that no competing interests exist.

## REFERENCES

1. Rezaei B, Taki M. Effects of tetrabutylammonium hydrogen sulfate as an electrolyte additive on the electrochemical behavior of lead acid battery. 2008;1663–1671. DOI: 10.1007/s10008-008-0547-x.
2. Liu W, Qin Q, Li D, Li G, Cen Y, Liang J. Lead recovery from spent lead acid battery paste by hydrometallurgical conversion and thermal degradation. Waste Manag. Res. 2020;38(3):263–270, 2020, DOI: 10.1177/0734242X19872263
3. Broda B, Inzelt G. Studying the effects of bismuth on the electrochemical properties of lead dioxide layers by using the in situ EQCM technique. J. Solid State Electrochem. 2020;24(11–12):2733–2739. doi: 10.1007/s10008-020-04569-3.
4. Zhao L, et al. Aqueous batteries as grid scale energy storage solutions. Renew. Sustain. Energy Rev. 2017;68(1):1174–1182. DOI: 10.1016/j.rser.2016.02.024.
5. Linden TBRD. Handbook of Batteries, 3rd ed. McGraw-Hill; 2001.
6. Lee J, Varela H, Uhm S, Tak Y. Electrodeposition of PbO<sub>2</sub> onto Au and Ti substrates. Electrochem. commun. 2000; 2(9):646–652. DOI: 10.1016/S1388-2481(00)00095-3.
7. Luk'yanenko TV, Shmychkova OB, Yanova CV, Krivonosova NI, Velichenko AB. The synthesis and electrocatalytic activity of PbO<sub>2</sub>-polyelectrolyte and PbO<sub>2</sub>-surfactant composite coatings. J. Chem. Technol. 2019;27(1):92–100. DOI: 10.15421/081910.
8. NŽ, EGD. Arminas Ilginis\*. Electrodeposition of Pb and PbO<sub>2</sub> on Graphite Felt in Membraneless Flow-Through Reactor: A Method to Prepare Lightweight Electrode Grids for Lead-Acid Batteries. Materials (Basel). 2021; 14(6122):1–14.
9. Suryanarayanan V, Nakazawa I, Yoshihara S, Shirakashi T. The influence of electrolyte media on the deposition/dissolution of lead dioxide on boron-doped diamond electrode - A surface morphologic study. J. Electroanal. Chem. 2006;592(2):175–182. DOI: 10.1016/j.jelechem.2006.05.010.
10. Mahalingam T, et al. Electrosynthesis and characterization of lead oxide thin films," Mater. Charact. SPEC. ISS. 2007;58(8-9):817–822. DOI: 10.1016/j.matchar.2006.11.021.
11. Casellato U, Cattarin S, Musiani M. Preparation of porous PbO<sub>2</sub> electrodes by electrochemical deposition of composites," Electrochim. Acta. 2003;48(27):3991–3998, DOI: 10.1016/S0013-4686(03)00527-9.
12. Velichenko A, Luk'yanenko T, Shmychkova O, Dmitrikova L. Electrosynthesis and catalytic activity of PbO<sub>2</sub>-fluorinated surfactant composites," J. Chem. Technol. Biotechnol. 2020;95(12): 3085–3092. DOI: 10.1002/jctb.6483.
13. Velichenko AB, Girenko DV, Danilov FI. Mechanism of lead dioxide electrodeposition," J. Electroanal. Chem. 1996;405(1–2):127–132. DOI: 10.1016/0022-0728(95)04401-9.
14. Yolshina LA, Kudyakov VY, Zyryanov VG. Development of an electrode for lead-acid batteries possessing a high electrochemical utilization factor and

- invariable cycling characteristics,” *J. Power Sources*. 1997;65(1–2):71–76.  
DOI: 10.1016/S0378-7753(97)02469-5.
15. Ji K, Xu C, Zhao H, Dai Z. Electrodeposited lead-foam grids on copper-foam substrates as positive current collectors for lead-acid batteries. *J. Power Sources*. 2014;248:307–316.  
DOI: 10.1016/j.jpowsour.2013.09.112.
  16. Hampson NA, Carr, Hampson . Lead dioxide electrode. 1972;157(1971).
  17. Kim Y. Information To Users Umi,” Dissertation. 2002;274.
  18. Velichenko A, Luk’yanenko T, Shmychkova O, Dmitrikova L. Electrosynthesis and catalytic activity of PbO<sub>2</sub>-fluorinated surfactant composites. *J. Chem. Technol. Biotechnol.* 2020;95(12): 3085–3092.  
DOI: 10.1002/jctb.6483.
  19. Cao M, Hu C, Peng G, Qi Y, Wang E. Selected-control synthesis of PbO<sub>2</sub> and Pb<sub>3</sub>O<sub>4</sub> single-crystalline nanorods. *J. Am. Chem. Soc.* 2003;125(17):4982–4983.  
DOI: 10.1021/ja029620l.
  20. Xi G, Peng Y, Xu L, Zhang M, Yu W, Qian Y. Selected-control synthesis of PbO<sub>2</sub> submicrometer-sized hollow spheres and Pb<sub>3</sub>O<sub>4</sub> microtubes. *Inorg. Chem. Commun.* 2004; 7(5):607–610.  
DOI: 10.1016/j.inoche.2004.03.001.
  21. Hossain MD, et al. Effects of additives on the morphology and stability of PbO<sub>2</sub> films electrodeposited on nickel substrate for light weight lead-acid battery application,” *J. Energy Storage*. 2020;27(2019):2020.  
DOI: 10.1016/j.est.2019.101108.
  22. Avijit Biswal C, MM, a, b, c Bankim Chandra Tripathy, a, b Tondepu Subbaiah, a, b Danielle Meyrick. Dual Effect of Anionic Surfactants in the Electrodeposited MnO<sub>2</sub> Trafficking Redox Ions for Energy Storage Dual Effect of Anionic Surfactants in the Electrodeposited MnO<sub>2</sub> Trafficking Redox Ions for Energy Storage. *J. of The Electrochem. Soc.* 2015;162,A30-A38.162:A30–A38.  
DOI: 10.1149/2.0191501jes.
  23. Egan DRP, Low CTJ, Walsh FC. Electrodeposited nanostructured lead dioxide as a thin film electrode for a lightweight lead-acid battery. *J. Power Sources*. 2011;196(13):5725–5730.  
DOI: 10.1016/j.jpowsour.2011.01.008.
  24. Taguchi M, Sugita H. Analysis for electrolytic oxidation and reduction of PbSO<sub>4</sub>/Pb electrode by electrochemical QCM technique. *J. Power Sources*. 2002;109(2):294–300.  
DOI: 10.1016/S0378-7753(02)00056-3.
  25. Ghasemi S, Mousavi MF, Shamsipur M. Electrochemical deposition of lead dioxide in the presence of polyvinylpyrrolidone. A morphological study. *Electrochim. Acta*. 2007;53(2):459–467.  
DOI: 10.1016/j.electacta.2007.06.068.
  26. Rufino ÉCG, Santana MHP, De Faria LA, Da Silva LM. Influence of lead dioxide electrodes morphology on kinetics and current efficiency of oxygen-ozone evolution reactions. *Chem. Pap.* 2010; 64(6):749–757.  
DOI: 10.2478/s11696-010-0062-2.
  27. Ghasemi S, Mousavi MF, Karami H, Shamsipur M, Kazemi SH. Energy storage capacity investigation of pulsed current formed nano-structured lead dioxide. *Electrochim. Acta*, 2006; 52(4):1596–1602.  
DOI: 10.1016/j.electacta.2006.02.068.
  28. Chen T, Huang H, Ma H, Kong D. Effects of surface morphology of nanostructured PbO<sub>2</sub> thin films on their electrochemical properties. *Electrochim. Acta*. 2013;88:79–85.  
DOI: 10.1016/j.electacta.2012.10.009.
  29. Yu N, Gao L, Zhao S, Wang Z. Electrodeposited PbO<sub>2</sub> thin film as positive electrode in PbO<sub>2</sub>/AC hybrid capacitor. *Electrochim. Acta*. 2009;54(14):3835–3841.  
DOI: 10.1016/j.electacta.2009.01.086.
  30. Zhang W, Tu CQ, Chen YF, Li WY, Houlachi G. Cyclic Voltammetric Studies of the Behavior of Lead-Silver Anodes in Zinc Electrolytes. 2013;22:1672–1679.  
DOI: 10.1007/s11665-012-0456-0.
  31. Ueda M, Watanabe A, Kameyama T, Matsumoto Y, Sekimoto M, Shimamune T. Performance characteristics of a new type of lead dioxide-coated titanium anode. *J. Appl. Electrochem.* 1995; 25(9):817–822.  
DOI: 10.1007/BF00233899.
  32. Ming Chen B, Cheng Guo Z, Wan Yang X, Dong Cao Y. Morphology of alpha-lead dioxide electrodeposited on aluminum substrate electrode. *Trans. Nonferrous Met. Soc. China (English Ed.)* 2010;20(1):97–103.  
DOI: 10.1016/S1003-6326(09)60103-5.
  33. He Z, Hayat MD, Huang S, Wang X, Cao P. Physicochemical Characterization of PbO<sub>2</sub> Coatings Electrothesized from a Methanesulfonate Electrolytic Solution. *J.*

- Electrochem. Soc. 2018;165(14):D670–D675.  
DOI: 10.1149/2.0161814jes.
34. Ruetschi P. Ruetschi1977. J. Power Sources, 2 3. 1977;2(1977178):3–24.
35. Hossain MD, Mustafa CM, Islam MM. Effect of deposition parameters on the morphology and electrochemical behavior of lead dioxide,” J. Electrochem. Sci. Technol. 2017;8(3):197–205.  
DOI: 10.5229/JECST.2017.8.3.197.
36. Nguyen TMP. Lead Acid Batteries in Extreme Conditions: Accelerated Charge, Maintaining the Charge With Imposed Low Current, Polarity Inversions Introducing Non-Conventional Charge Methods. HAL, Arch. Ouvert. 2009;175.
37. Kong J, Shi S, Kong L, Ni J. Preparation and characterization of PbO<sub>2</sub> electrodes doped with different rare earth oxides. Electrochim. Acta. 2007;53(4):2048–2054.  
DOI: 10.1016/j.electacta.2007.09.003.

---

© 2022 Yasmin et al.; This is an Open Access article distributed under the terms of the Creative Commons Attribution License (<http://creativecommons.org/licenses/by/4.0>), which permits unrestricted use, distribution, and reproduction in any medium, provided the original work is properly cited.

*Peer-review history:*  
*The peer review history for this paper can be accessed here:*  
<https://www.sdiarticle5.com/review-history/84895>